BULLETIN OF THE POLISH ACADEMY OF SCIENCES
TECHNICAL SCIENCES, Vol. 69(6), 2021, Article number: e139204
DOI: 10.24425/bpasts.2021.139204

Determining horizontal curvature of railway track axis in mobile satellite measurements

Władysław KOC[1*], Andrzej WILK[1], Cezary SPECHT[2], Krzysztof KARWOWSKI[1], Jacek SKIBICKI[1], Krzysztof CZAPLEWSKI[2], Slawomir JUDEK[1], Piotr CHROSTOWSKI[3], Jacek SZMAGLIŃSKI[3], Paweł DĄBROWSKI[2], Mariusz SPECHT[2], Sławomir GRULKOWSKI[3], and Roksana LICOW[3]

[1] Gdańsk University of Technology, Faculty of Electrical and Control Engineering, ul. G. Narutowicza 11/12, 80-233 Gdańsk, Poland
[2] Gdynia Maritime University, Faculty of Navigation, al. Jana Pawła II 3, 81-345 Gdynia, Poland
[3] Gdańsk University of Technology, Faculty of Civil and Environmental Engineering, ul. G. Narutowicza 11/12, 80-233 Gdańsk, Poland

Abstract. The article discusses the applicability of a novel method to determine horizontal curvature of the railway track axis based on results of mobile satellite measurements. The method is based on inclination angle changes of a moving chord in the Cartesian coordinate system. In the presented case, the variant referred to as the method of two virtual chords is applied. It consists in maneuvering with only one GNSS (Global Navigation Satellite System) receiver. The assumptions of the novel method are formulated, and an assessment of its application in the performed campaign of mobile satellite measurements is presented. The shape of the measured railway axis is shown in the national spatial reference system PL-2000, and the speed of the measuring trolley during measurement is calculated based on the recorded coordinates. It has been observed that over the test section, the curvature ordinates differ from the expected waveform, which can be caused by disturbances of the measuring trolley trajectory. However, this problem can easily be overcome by filtering the measured track axis ordinates to obtain the correct shape – this refers to all track segments: straight sections, circular arcs and transition curves. The virtual chord method can also constitute the basis for assessing the quality of the recorded satellite signal. The performed analysis has shown high accuracy of the measuring process.

Key words: GNSS measurements; railway track axis; horizontal curvature; moving chord method application; accuracy assessment.

1. INTRODUCTION

Determining main geometric parameters of the railway track in the horizontal plane (positions and lengths of straight track sections, positions, radii and lengths of circular arcs, and positions, types and lengths of transition curves) is a basic operation in the process of railway track shape evaluation. Railway track measurement methods which are in use in different countries [1–7] can boast a very long tradition, but – despite various innovations being introduced – they can still be characterized by massive labor consumption, with the associated huge financial expenses.

New possibilities in the field of inventory of engineering objects are created by the development of satellite measurements and an increase in the accuracy of measurements based on the Global Navigation Satellite System (GNSS) [8–12]. In Poland, the method of mobile satellite measurements (Fig. 1) has been developed for over a decade [13–20]. The aim of the ongoing BRIK research project [21, 22] is to obtain an implementation solution.

As a result of measurements, a set of figures is obtained which, after relevant postprocessing, compose a set of coordinates in a given Cartesian system (in Poland – with respect to the horizontal plane – the national spatial reference system PL-2000). The collected set of coordinates makes up the basis for identifying individual geometric elements of the track. The method traditionally used for this purpose is based on the chart of horizontal sagittas (Fig. 2), being the most frequently used tool for assigning track points to sections with defined geometry.

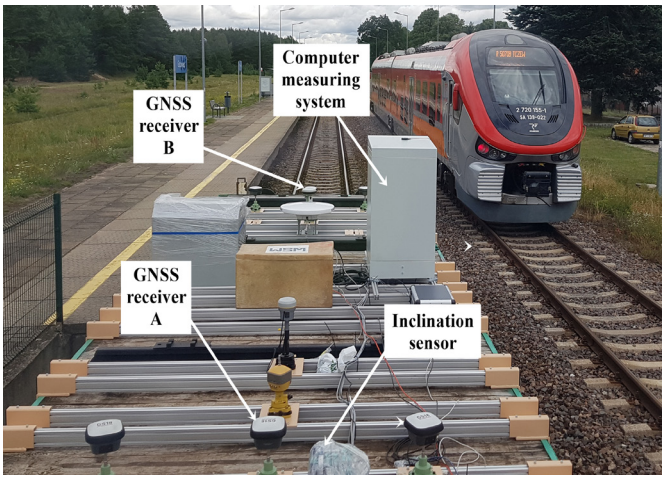

Fig. 1. The measuring platform during mobile satellite measurements; GNSS (Global Navigation Satellite System) receivers A and B define the baseline vector of the platform

*e-mail: kocwl@pg.edu.pl

Manuscript submitted 2021-04-14, revised 2021-09-02, initially accepted for publication 2021-09-05, published in December 2021

Fig. 2. An example of the chart of horizontal sagittas obtained with an electronic track gauge (on the horizontal axis – distance (m), on the vertical axis – sagitta values (mm), the red lines indicate the tolerance limits for the speed 50 km/h)

The sagitta chart method is still very popular in railway applications. Since the sagitta diagram is very similar to the curvature diagram, this method is sometimes used for determining the railway track curvature, which seems unjustified from the formal point of view. It is noteworthy that for years the measurement of sagittas (horizontal and vertical ones) has constituted the basis of diagnostic methods to evaluate the geometric condition of a railway track [23–27]. The terms "horizontal unevenness chart" and "vertical unevenness chart" used in those measurements mean, in fact, the charts of sagittas measured on a given rail. A similar situation can be observed in commercial computer programs supporting inter alia railway track designing, [28–30].

It is noteworthy that the measurement of horizontal sagittas is done in the linear coordinate system, while the railway track is described by point coordinates in the Cartesian coordinate system (which results from requirements concerning track axis marking, among other reasons). Transformation from linear to Cartesian coordinates is difficult and may lead to problems in interpretation of the given geometric structure. Therefore, it is advisable to perform railway track shape identification in the Cartesian system. This recommendation would undoubtedly undermine the sense of further use of the sagitta chart method for this purpose, provided that a direct method to determine curvature is available.

2. DETERMINING CURVATURE WITH THE MOVING CHORD METHOD

The definition of curvature imposes the need to operate with inclination angles of tangents to the geometric system. When the analytical description of a given curve is known, this does not pose a problem. However, for the real railway track, most frequently deformed as result of its operation, determining tangents can be troublesome and burdened with relatively large errors, therefore a concept has emerged to operate with chords instead of tangents when determining track curvature. In [31], a theoretical method was proposed which made use of inclination angle changes of a moving chord of given length (so-called moving chord method) to determine curvature. The use of analytical notation enabled precise positioning of chord ends. The method was then practically verified on selected geometric layouts. Figure 3 shows a schematic diagram of determining curvature with the proposed method.

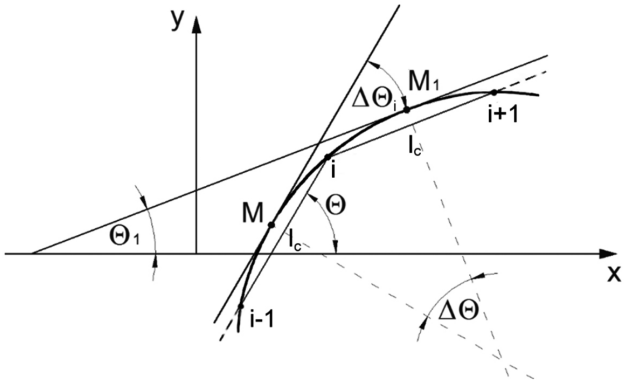

Fig. 3. Schematic diagram of determining curvature with the moving chord method [31]

In the moving chord method, it was assumed that for the small railway track segment under consideration, the tangents (derived at points M and M_1 in Fig. 3) and the corresponding chords (sections $(i-1)\div i$ and $i\div(i+1)$) are parallel to each other, while the tangency points are projected perpendicularly onto the chord centers. Curvature k_i at point i is calculated from the following formula:

$$k_i = \frac{\Delta\theta_i}{l_c}, \tag{1}$$

where l_c is the chord length, and angle $\Delta\theta_i$ is the difference between the inclination angles of two adjacent chords with common point i, i.e.

$$\Delta\theta_i = \theta_{i\div(i+1)} - \theta_{(i-1)\div i}\,. \tag{2}$$

The use of this procedure requires information about curve coordinates in the Cartesian reference system, as the values of angles $\theta_{(i-1)\div i}$ and $\theta_{i\div(i+1)}$ correspond to gradients of straight lines describing both chords.

In [31], the proposed method to determine curvature was verified on an unambiguously defined elementary geometric layout of the railway track, which consisted of a circular arc and two symmetrically arranged transition curves of the same type and length. The track segment selected for verification had been calculated based on principles of the analytical design method [32]. A number of geometric variants were analyzed for different train speeds, types of applied transition curves and track diversion angles. Full compatibility was observed between the obtained curvature values and those used as the basis for designing the geometry of the analyzed track segment, with respect to both the circular arc, and the transition curves. A possibility was also indicated to use the proposed method when determining curvature with respect to both the X-axis in the Cartesian system, and the length parameter in the linear system.

It was also noted that the proposed method has a wide applicability potential. The practical aspect of the present analysis may be identified when geometrical characteristics of the track axis determined from measurements are not known and the basic goal is to determine them. In this situation, the proposed method ideally meets the assumptions of mobile satellite measurements, as these measurements provide an extensive number of track axis coordinates in the Cartesian coordinate system in a very short time.

In [31], an analytical record of the geometric systems in question was available, so determining the Cartesian coordinates of the ends of the chord directed backwards and forwards did not pose a problem. In this situation, it was easy to determine the values of the respective slope angles $\theta_{(i-1)\div i}$ and $\theta_{i\div(i+1)}$. When determining the curvature of the track on the basis of measurement data, the coordinates of the track axis are discrete and it would be difficult to create an analytical record of them. Therefore, it is necessary in such a case to adapt the discussed moving chord method to the adopted measurement procedure. This issue lies at the heart of this article.

3. VARIANT OF TWO VIRTUAL CHORDS

3.1. Applicability of the moving chord method

In mobile satellite measurements, the characteristics of the geometric layout under consideration and its mathematical notation are unknown. Hence, the essential problem concerns determining endpoint coordinates of the two adjacent chords, because they cannot be determined analytically. As the measurement points are discrete, the position of the ends of the chords should be found via interpolation at relevant intervals. The basic goal, which is determining the track curvature, can be obtained in various manners, of which two application variants of the moving chord method appear to be most effective:

- the variant making use of the fixed base of the measuring trolley, and
- the two virtual chords variant.

When using the measuring platform with two satellite receivers installed at bogie pivot pin points, the positions of the satellite antennas define the so-called fixed base of the trolley. This fixed base can be used as the measuring chord in the moving chord method. The main advantage of operating with a fixed base is that the records from both satellite antennas come at the same time, under the same conditions (measuring speed, visibility of satellites). This eliminates situations in which we have to deal with coordinates measured at different times, in the presence of different factors which might affect accuracy. In the BRIK project [21, 22], the fixed base method will be the basic method to determine the railway track axis curvature.

However, in some situations, the need to use data from two satellite antennas may generate certain limitations. Moreover, the operation of the antennas can be affected by disturbances, as a result of which the distance between them calculated from measurements will not be equal to the nominal length of the fixed base (some real situations were recorded where such inequality took place).

Therefore, when the use of coordinates recorded exactly at the same time is not necessary and, simultaneously, we can ensure preserving constant measuring speed, it seems advisable to consider making use of data from only one satellite antenna. This means the necessity to use two virtual chords created forward and backward from point i (looking in the direction of the measuring run). This solution has an additional advantage which may be of high importance in some situations: different chord lengths can be assumed, which may prove extremely useful when determining border points between different geometric elements of the track. The fixed base method does not offer such an opportunity.

In this work, intended to analyze the results obtained in the selected measuring campaign, the method based on the use of only one GNSS antenna is applied.

3.2. Assumptions of the method to determine railway track curvature

In the conducted research, the full data set for the measuring point comprises:

- time of measurement t_i,
- horizontal eastward coordinate Y in PL-2000 coordinate system,
- horizontal northward coordinate X in PL-2000 coordinate system,
- vertical coordinate Z in relevant spatial system,
- inclination angle α_v in longitudinal profile,
- inclination angle α_t in lateral section.

In the first step, the recorded track axis coordinates should be corrected using angles α_v and α_t measured with inclinometers [33, 34] or by means of an inertial system. Then, these results can be used for reconstructing the existing position of the railway track axis. When determining the horizontal curvature,

this should be done using the corrected horizontal coordinates $Y(t_i)$ and $X(t_i)$.

All measuring points have their index numbers $i = 1, 2, \ldots, n$. We start determining curvature k_i from point i situated in such a way that a virtual chord of length l_c can be projected backward. Likewise, the calculations should end at point i from which the virtual chord, of the same length, can still be projected forward.

The basic operation to be performed is finding index numbers of points defining the intervals in which endpoints of virtual chords projected from point i are situated. For the rear chord, this interval is given by points q_i (defining the boundary of the interval further from point i) and $q_i + 1$ (defining the boundary of the interval less distant from point i). In the case of the front chord, these are points $p_i - 1$ (defining the boundary of the interval less distant from point i) and p_i (defining the boundary of the interval further from point i). These limiting points are found by checking the distances of successive points from point i in the direction of increasing and decreasing index numbers. For the rear chord these distances are determined from the formula below:

$$l_{(i-k)\div i} = \sqrt{(Y_i - Y_{i-k})^2 + (X_i - X_{i-k})^2} \tag{3}$$

and for the front chord from the following formula:

$$l_{i\div(i+k)} = \sqrt{(Y_i - Y_{i+k})^2 + (X_i - X_{i+k})^2}, \tag{4}$$

where $k \varepsilon N_+$.

After each calculation step, we check whether the condition $l_{(i-k)\div i} \geq l_c$ is met for the rear chord and $l_{i\div(i+k)} \geq l_c$ for the front chord. The first value $i-k$ for the rear antenna which meets the above condition is marked as q_i, while for the front antenna, the first value $i+k$ is marked as p_i.

Since, unlike the fixed base method, the considered variant of the moving chord method omits the time parameter and instead makes use of measuring point index numbers, it seems profitable to maintain similar distances between adjacent points. This is equivalent to the requirement to take measurements at constant speed of the measuring trolley.

Once the coordinates Y_{q_i}, X_{q_i} and $Y_{q_{i+1}}$, $X_{q_{i+1}}$ of points limiting the interval in which the endpoint of the rear antenna is situated are known, the distances of these points from point i can be calculated:

$$l_{q_i} = \sqrt{(Y_i - Y_{q_i})^2 + (X_i - X_{q_i})^2}, \tag{5}$$

$$l_{q_{i+1}} = \sqrt{(Y_i - Y_{q_{i+1}})^2 + (X_i - X_{q_{i+1}})^2}. \tag{6}$$

These data make it possible to determine the coordinates of the rear chord endpoint, i.e. point B_i, using the following formulas:

$$Y_{B_i} = Y_{q_{i+1}} + \frac{l_c - l_{q_{i+1}}}{l_{q_i} - l_{q_{i+1}}} \left(Y_{q_i} - Y_{q_{i+1}}\right), \tag{7}$$

$$X_{B_i} = X_{q_{i+1}} + \frac{l_c - l_{q_{i+1}}}{l_{q_i} - l_{q_{i+1}}} \left(X_{q_i} - X_{q_{i+1}}\right). \tag{8}$$

The gradient of the straight line passing through points B_i and i and representing the rear chord is as follows:

$$s_{B_i\div i} = \frac{X_i - X_{B_i}}{Y_i - Y_{B_i}}. \tag{9}$$

If $s_{B_i\div i} > 0$, then the inclination angle of the fixed base is $\theta_{B_i\div i} \in \left\langle 0, \frac{\pi}{2} \right\rangle$ and is given in the Y, X coordinate system by the formula below:

$$\theta_{B_i\div i} = \operatorname{atan} \frac{X_i - X_{B_i}}{Y_i - Y_{B_i}}. \tag{10}$$

If $s_{B_i\div i} < 0$, then the inclination angle of the fixed base is $\theta_{B_i\div i} \in \left\langle \frac{\pi}{2}, \pi \right\rangle$ and is given by the formula below:

$$\theta_{B_i\div i} = \pi + \operatorname{atan} \frac{X_i - X_{B_i}}{Y_i - Y_{B_i}}. \tag{11}$$

Inclination angle of the front chord is determined analogously. Based on the known coordinates Y_{p_i}, X_{p_i} and Y_{p_i-1}, X_{p_i-1} of points limiting the interval in which the endpoint of the front antenna is situated, the distances l_{p_i} and l_{p_i-1} of these points from point i can be calculated. These data make it possible to determine the coordinates of the front chord endpoint, i.e. point F_i. The gradient of the straight line passing through points i and F_i and representing the front chord is:

$$s_{i\div F_i} = \frac{X_{F_i} - X_i}{Y_{F_i} - Y_i}. \tag{12}$$

If $s_{i\div F_i} > 0$, then the inclination angle of the fixed base is $\theta_{i\div F_i} \in \left\langle 0, \frac{\pi}{2} \right\rangle$ and is given by the formula below:

$$\theta_{i\div F_i} = \operatorname{atan} \frac{X_{F_i} - X_i}{Y_{F_i} - Y_i}. \tag{13}$$

If $s_{i\div F_i} < 0$, then the inclination angle of the fixed base is $\theta_{i\div F_i} \in \left\langle \frac{\pi}{2}, \pi \right\rangle$ and is given in the Y, X coordinate system by the formula below:

$$\theta_{i\div F_i} = \pi + \operatorname{atan} \frac{X_{F_i} - X_i}{Y_{F_i} - Y_i}. \tag{14}$$

3.3. Curvature value at point *i*

The curvature value at point i is given by the following formula:

$$k_i = \pm \left| \frac{\theta_{i\div F_i} - \theta_{B_i\div i}}{l_c} \right|. \tag{15}$$

The sign "+" in (15), meaning positive curvature, corresponds to the situation when convexity along the length of the curve is directed downwards, while the negative value – to the convexity directed upwards.

The virtual chord method is undoubtedly simpler in calculations than that making use of the fixed base of the measuring trolley. However, it should be kept in mind that it is extremely sensitive to measuring speed disturbances and the need to operate on data sets recorded at different times. Therefore, it should

be used locally, when the use of the fixed base method proves ineffective, or when we want to use shorter chords for determining the border points between geometric elements more precisely. In this work, the virtual chord method was also used to assess the efficiency of the applied measuring technique.

4. ASSESSING THE CURVATURE CALCULATION PROCESS IN MOBILE SATELLITE MEASUREMENTS

4.1. Test segment

The analyzed test segment comprises a fragment of a single-track railway line, of about 4.7 km in length. The measurement was conducted using the GNSS receivers of 100 Hz frequency, installed on a four-axis trolley, at the front bogie pivot point (looking in the direction of motion). The trajectory of this railway line fragment recorded in mobile satellite measurements is shown in Fig. 4, in the PL-2000 coordinate system.

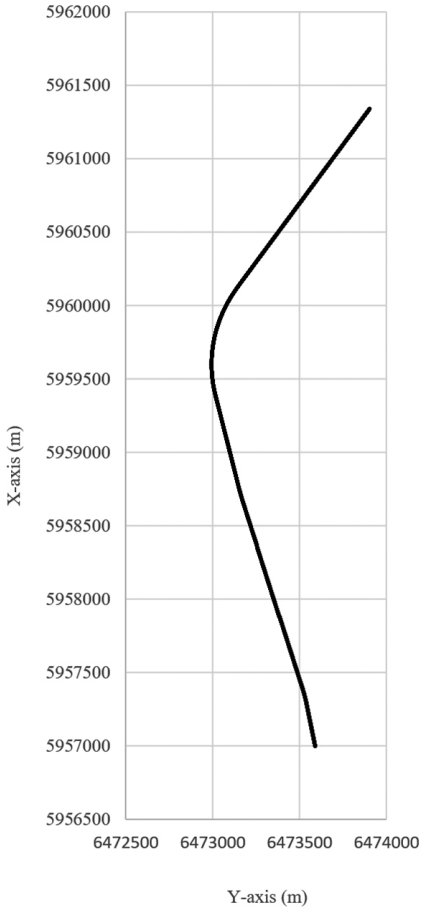

Fig. 4. Railway track trajectory recorded in mobile satellite measurements

For further analysis, we should move to the linear system, i.e. calculate the distances of successive measuring points from a given starting point – the so-called L variable. The starting point will be denoted as $i = 1$.

The distance between two adjacent measuring points is:

$$\Delta L_{i\div i+1} = \sqrt{(Y_{i+1} - Y_i)^2 + (X_{i+1} - X_i)^2}\,. \tag{16}$$

The linear coordinate L_i, being the distance of the given point i from point $(Y_1,\ X_1)$, is calculated from the following formula:

$$L_i = \sum_{i=1}^{i=n-1} \Delta L_{i\div i+1}\,. \tag{17}$$

Equation (17) makes use of coordinates of all points situated along both the straight sections and arcs. As a consequence, the measuring errors sum up in the calculation procedure. For straight sections, the L_i variable assessment error can be substantially reduced by calculating the distance directly from the starting point, taking two extreme points into account. In this case, the following formula is applicable:

$$L_i = \sqrt{(Y_i - Y_1)^2 + (X_i - X_1)^2}\,. \tag{18}$$

The linear coordinate L enables finding locations of particular geometric elements based on the determined railway track axis curvature, as well as calculating the track mileage. Moreover, in combination with the measured height coordinate Z it can be used for determining the longitudinal profile of the track.

4.2. Determining measuring trolley speed during measurement

In mobile satellite measurements, the measurements of railway track axis coordinates are taken at fixed time intervals resulting from the frequency of the installed GNSS receivers. For $f = 100$ Hz, the time interval between two successive measurements is 10 ms. Since the distance between two successive measuring points is known, the speed of the measuring trolley in this interval can be directly calculated. This speed (in km/h) is given by the formula below:

$$V_{i\div i+1} = 3.6 f \Delta L_{i\div i+1}\,. \tag{19}$$

For straight sections, (19) can be replaced by its modified form:

$$V_{i\div i+1} = 3.6 f\,(L_{i+1} - L_i)\,. \tag{20}$$

where the values of L_i and L_{i+1} are calculated from (18).

Figure 5 shows the measuring speed waveform $V(L)$ covering initial 300 m of the test segment, as calculated from (20). The assumed starting point had coordinates $Y_1 = 6473899.914$ m and $X_1 = 5961334.294$ m, and was situated on a straight section being the upper part of the trajectory shown in

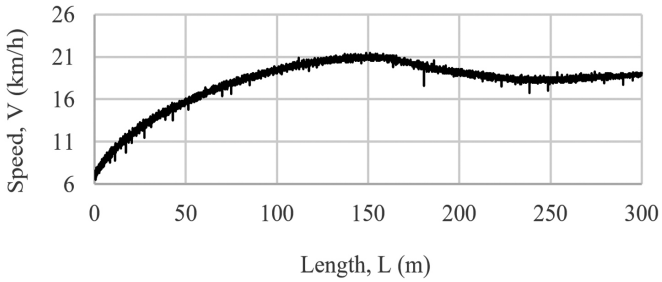

Fig. 5. Speed of measuring trolley over initial 300 m of the test segment, calculated from the measured Cartesian coordinates

Fig. 4 (the motion of the measuring trolley was in the direction of decreasing X values).

What is noteworthy here is the high precision of speed value calculations, which is undoubtedly related to precision in determining distances between successive measuring points. This issue will be discussed in detail in Section 4.4. The very high accuracy of determining distance $\Delta L_{i\div(i+1)}$ is indicated by the values of standard deviation $\sigma_{\Delta L}$ given in Table 1. In the vast majority of cases these values do not exceed 0.5 mm.

A similar situation as that observed in Fig. 5 with respect to the accuracy had taken place over further 1400 m, until radical deterioration of quality of the recorded GNSS signal was observed. This issue will be discussed in greater detail in the next section.

4.3. Determining horizontal curvature

Horizontal curvature k_i at consecutive measuring points was calculated from (15) assuming chord length $l_c = 7$ m, equal to the fixed base of the measuring trolley. On straight sections, the linear coordinate was calculated from (18), while on arcs – from (17). The results of these calculations enabled drawing the curvature waveform over the geometric layout length.

Figure 6 shows the railway track curvature over the initial 10 m of the test segment. The measurement was taken at increasing speed of the measuring trolley (see Fig. 5). As can be observed, the curvature waveform differs radically from $k(l)$ diagrams presented for model systems in [31]. In that case, full compatibility of the curvature obtained using the moving chord method with the theoretical waveform was observed, while in

Table 1
Compilation of $\Delta L_{i\div(i+1)}$ statistics in successive speed classes

n_c	L_p [m]	L_k [m]	$\Delta L_{p\div k}$ [m]	$n_{p\div k}$	$\overline{V_{j\div j+1}}$ [km/h]	σ_V [km/h]	$\overline{\Delta L_{j\div j+1}}$ [mm]	$\sigma_{\Delta L}$ [mm]	$\sigma_{\Delta L}/\overline{\Delta L}$ [%]
142	782.661	798.218	15.557	315	17.836	0.121	49.548	0.336	0.678
141	806.111	827.448	21.337	429	17.947	0.131	49.855	0.365	0.782
140	739.219	748.570	9.351	188	18.054	0.143	50.152	0.397	0.791
139	849.331	854.130	4.799	96	18.186	0.106	50.519	0.294	0.581
138	234.663	254.909	20.246	399	18.313	0.211	50.877	0.598	1.175
137	876.690	884.695	8.005	157	18.471	0.174	51.311	0.482	0.939
136	895.504	909.341	13.838	269	18.588	0.133	51.635	0.369	0.716
135	917.328	923.675	6.347	123	18.730	0.115	52.031	0.319	0.614
134	930.727	942.520	11.792	226	18.868	0.120	52.413	0.334	0.638
133	949.838	959.131	9.293	177	19.016	0.125	52.824	0.346	0.656
132	968.517	981.937	13.420	253	19.171	0.108	53.253	0.299	0.562
131	1624.722	1682.390	57.668	1076	19.294	0.164	53.594	0.456	0.851
130	611.935	644.452	32.517	589	19.477	0.126	54.104	0.350	0.648
129	527.548	604.717	77.169	1417	19.619	0.125	54.501	0.348	0.638
128	433.603	519.181	85.578	1561	19.761	0.163	54.898	0.457	0.833
127	1059.762	1076.095	16.333	296	19.931	0.126	55.366	0.351	0.635
126	1083.150	1106.612	23.462	422	20.063	0.106	55.731	0.295	0.530
125	1118.266	1136.733	18.449	329	20.248	0.116	56.246	0.322	0.573
124	1141.307	1309.644	168.337	2974	20.384	0.142	56.625	0.399	0.704
123	1316.700	1323.441	6.741	119	20.567	0.126	57.132	0.348	0.609
122	1330.499	1335.160	4.661	82	20.718	0.115	57.551	0.320	0.556
121	142.111	157.926	15.815	272	20.929	0.203	58.150	0.559	0.961
120	1357.293	1362.386	5.093	88	21.091	0.174	58.589	0.485	0.828
119	1370.975	1374.640	3.665	63	21.283	0.141	59.121	0.390	0.659
118	1381.700	1385.748	4.048	69	21.431	0.105	59.531	0.292	0.491
117	1392.811	1397.135	4.324	73	21.645	0.224	60.126	0.631	1.050
116	1404.198	1414.871	10.673	177	21.832	0.125	60.645	0.346	0.570
115	1421.932	1451.461	29.529	484	22.010	0.148	61.138	0.412	0.674
114	1461.224	1490.098	28.874	470	22.163	0.158	61.564	0.439	0.713

Fig. 6 the curvature ordinates $k(L)$ differ visibly from the curvature $k = 0$ expected on the straight section. This may be caused by track deformations resulting from its exploitation, but the main cause seems to be the disturbances of measuring trolley trajectory occurring during the measurement. Entering of wheelsets into the track generates lateral displacements of the trolley with the satellite receiver installed on its bogie pivot. The recorded deviations are not random in nature, but reveal certain regularity. The diagram in Fig. 6 was obtained based on data from over 400 measuring points.

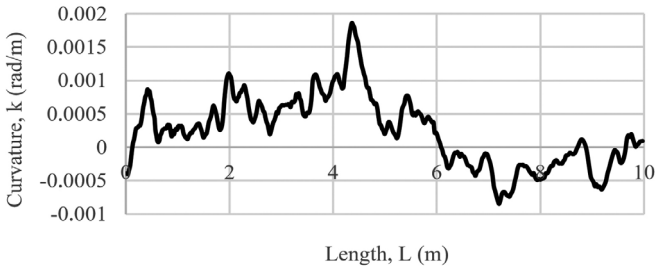

Fig. 6. Track curvature over initial 10 m of the test segment

However, this irregularity is not a problem from the point of view of the basic goal of the performed measurements, i.e. determining the curvature of the given geometric layout. This can easily be confirmed by analyzing the curvature waveform for a longer track segment (Fig. 7).

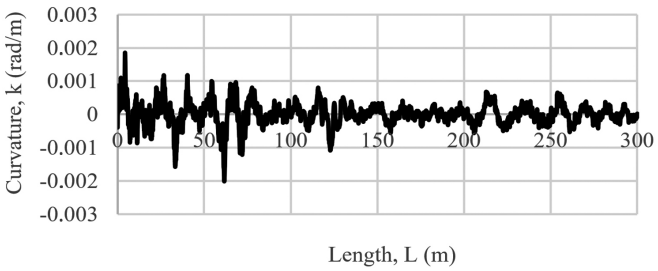

Fig. 7. Track curvature over initial 300 m of the test segment, calculated based on mobile satellite measurements

Figure 7 shows the track curvature over initial 300 m of the test segment. As can be seen, deviations from zero curvature decrease as a result of speed stabilization at a given level (see Fig. 5). However, from the practical point of view, of highest importance is that it is sufficient to filter curvature ordinates to obtain the correct track shape [35], as in this case there is no doubt that the presented fragment of the test segment is straight and its curvature is $k = 0$. This was confirmed by $k(L)$ diagrams drawn for further fragments of the test segment.

The $k(L)$ ordinates also need filtering on circular arcs and transition curves. It results from the curvature waveform in the transition curve region (Fig. 8) that these ordinates oscillate around some constant value; we can also assume that the transition from straight section to arc is linear. Filtering out high frequencies enables determining endpoints of the transition curve (and, consequently, its length) as well as the radius of the circular arc.

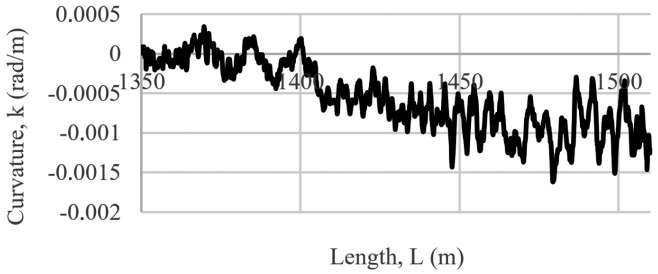

Fig. 8. Curvature waveform in the transition curve region, calculated based on mobile satellite measurements

The horizontal curvature waveform determined by means of the virtual chord method may also become the basis for assessing the quality of the recorded satellite signal. This possibility is illustrated in Fig. 9 and Fig. 10. At some time during the measurement session, for $L \approx 1725$ m, rapid deterioration in satellite signal quality was recorded, which can be observed as visible increase of deviations from the mean value on both the curvature waveform (Fig. 9) and the speed waveform (Fig. 10). Hence, the virtual chord method makes it possible to detect unfavorable situations caused by disturbances in signal recording and, consequently, to indicate the need to introduce corrections to the mobile satellite measurement procedure in a given track fragment.

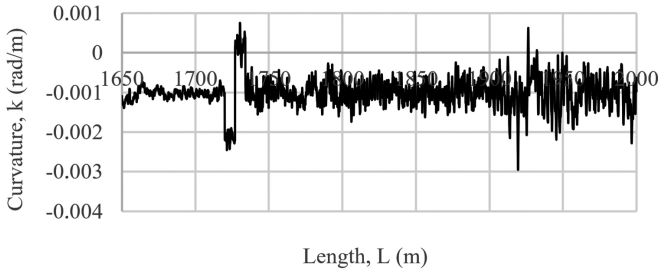

Fig. 9. Curvature waveform illustrating satellite signal quality deterioration

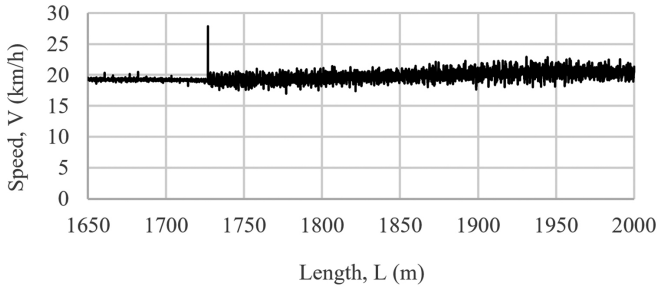

Fig. 10. Speed of measuring trolley in the region of satellite signal quality deterioration

4.4. Coordinate determination accuracy

Increasing the accuracy and availability of GNSS measurements is one of the major study areas. Mobile satellite measurements on the rail track conducted in 2009–2015 focused on the availability assessment for three accuracy levels, which are

required for carrying out individual construction and geodesy-related tasks in railway engineering. These include [13]:

- deformation accuracy (dd) – enabling one to identify the place and extent of rail track deformations, for which the maximum horizontal position error was adopted as not exceeding 1 cm,
- inventory accuracy (di) – applied in rapid stocktaking of existing rail tracks, for which the maximum horizontal position error was adopted as not exceeding 3 cm,
- design accuracy (dp) – applied in design and construction work, for which the maximum horizontal position error was adopted as not exceeding 10 cm.

It should be emphasized that the above-mentioned three levels of accuracy have been defined on the basis of experience gained during the implementation of GNSS inventory measurements of railway tracks in 2009–2015 and do not result from any norms or standards. In the years 2009–2011, in the research on the availability of high-precision position coordinates, GNSS networks based only on the GPS system were used, for which the availability of deformation accuracy was only 3.91%, inventory accuracy was 66.39% and design accuracy – 68.14%. In subsequent studies (in 2014), two-system networks (GPS/GLONASS) were used, achieving deformation accuracy of 54.48%, inventory accuracy of 89.53% and design accuracy of 93.22%. However, in the research conducted in 2015, during which multi-system networks were used, without the use of the Inertial Navigation System (INS), the following accuracy was obtained: $dd = 56.75\%$, $di = 83.15\%$ and $dp = 85.39\%$, and while using INS system – $dd = 88.03\%$, $di = 100\%$ and $dp = 100\%$. This clearly proves the suitability of mobile satellite measurements for the purposes of stocktaking the railway track.

The BRIK project [21, 22] included verification of satellite railway track measurements combined with standard geodetic methods [36]. As it turned out, the presented virtual chord method also offers some possibilities concerning the accuracy of the obtained results. The basis for this accuracy evaluation can be the analysis of distances between two adjacent measuring points, provided by (16).

The values of $\Delta L_{i\div(i+1)}$ certainly differ, depending on local speed on the measuring trolley. Therefore, comparing them can only make sense for a given speed interval (class). It has been assumed that the speed class is given by the number of measuring points situated over the virtual chord length (the same for both chords), and the greater the number of these points, the lower the speed on the track fragment being considered.

For each speed class of $\Delta L_{i\div(i+1)}$ values, the mean values and standard deviations were calculated. The results are collated in Table 1, ordered with respect to the decreasing number of measuring points in the speed class. The following symbols are adopted in Table 1: n_c – number of points defining the speed class, L_p and L_k – endpoint coordinates of the given speed interval, $\Delta L_{p\div k}$ – length of the speed interval, $n_{p\div k}$ – number of measuring points in the interval, $\overline{V_{i\div(i+1)}}$ – mean speed, σ_V – standard deviation of speed, $\overline{\Delta L}_{i\div(i+1)}$ – average distance between two adjacent measuring points, $\sigma_{\Delta L}$ – standard deviation of the distance between adjacent points.

It results from Table 1 that the lengths of the intervals comprising a given speed class differ distinctly. However, regardless of the length of a given speed interval (corresponding to the number of measuring points composing it), a very clear view of the situation has been obtained. Although in each speed class, the values of $V_{i\div(i+1)}$ and $\Delta L_{i\div(i+1)}$ differ, their mean values increase gradually and steadily with decreasing n_c.

The most surprising result of this analysis were the obtained values of standard deviation of the distance between two adjacent measuring points. In nearly all cases, these deviation values did not exceed 0.5 mm and 1% of the mean value. From the point of view of GNSS measurement accuracy assessment, this result is of fundamental importance, as it contradicts traditional skepticism concerning applicability of these measurements. However, one basic condition should be met in the entire measuring procedure – the measurements should be properly planned and conducted. The analysis presented in the paper confirms the potential of the applied measuring method, simultaneously indicating potential threats. Rapid quality deterioration of the received signal, shown in Fig. 9 and Fig. 10, which took place during the measuring session, persisted until the end of measurement and led to the increase of $\sigma_{\Delta L}$ by several times.

5. SUMMARY

In engineering practice, the type and characteristics of the horizontal curvature existing on a given geometric track layout are most frequently identified indirectly – based on the values of sagittas measured from the chord stretched along the track. Radical improvement in this situation is expected to be brought about by the method of mobile satellite measurements, developed in Poland for over a decade now. The aim of the ongoing BRIK research project is to obtain an implementation solution.

Further use of the sagitta chart method would soon become obsolete if there existed a direct method to determine curvature. In [31], the assumptions of the novel method to determine horizontal curvature were formulated. This method is based on inclination angle changes of a moving chord in the Cartesian coordinate system. It was verified on an unambiguously defined elementary geometric layout of the railway track. The proposed method may prove extremely applicable when geometrical characteristics of the track axis calculated from measurements are not known and the basic goal is to determine them.

In the article, applicability of the moving chord method was analyzed. The applied variant of this method, referred to as the method of two virtual chords, consists in maneuvering with only one GNSS receiver. The assumptions of the method to determine railway track axis curvature were given, along with the assessment of its application in the performed campaign of mobile satellite measurements. The measured track axis was shown in the PL-2000 coordinate system. Based on the measured coordinates, the speed of the measuring trolley during the measurement was calculated.

Basic activities aimed at determining the horizontal curvature of the track. As it turned out, the obtained $k(L)$ waveforms differed radically from those presented for model systems [31],

where full compatibility was observed between the obtained curvature values and those used as the basis for designing the geometry of the analyzed track segment. This might be caused by track deformations resulting from its exploitation, but the main cause seems to be measuring trolley trajectory disturbances taking place during the measurement. However, in practice, this problem can easily be overcome by filtering the measured track axis ordinates to obtain the correct shape – this refers to all track segments: straight sections, circular arcs and transition curves.

The virtual chord method can also become the basis for quality assessment of the satellite signals received. During the measuring session, rapid deterioration in satellite signal quality was observed in the form of visible increase of deviations from the mean value on both the curvature waveform and the speed waveform. The procedure adopted for assessing the obtained accuracy involved the analysis of distances between two adjacent measuring points. For the interval of correct operation of satellite receivers, the performed analysis gave a clear and logical view of the existing situation. The most surprising result of this analysis were the calculated values of standard deviation of the distance between points. In nearly all cases, these deviation values did not exceed 0.5 mm and 1% of the mean value. From the point of view of GNSS measurement accuracy assessment, this result is of fundamental importance, as it contradicts traditional skepticism concerning applicability of these measurements.

ACKNOWLEDGEMENTS

The authors would like to thank the National Centre for Research and Development in Warsaw and the Polish Railway Lines for financing the research.

REFERENCES

[1] *British railway track design, construction and maintenance*. 6th ed., The Permanent Way Institution, London, UK, 1993.

[2] *883.2000 DB_REF-Festpunktfeld*, DB Netz AG, Berlin, Germany, 2016.

[3] *Railway applications—Track—Track alignment design parameters—Track gauges 1435 mm and wider—Part 1: Plain line*, EN 13803-1, CEN, Brussels, Belgium, 2010.

[4] *Code of federal regulations title 49 transportation*, US Government Printing Office, Washington, DC, USA, 2008.

[5] *Standard: Railway Surveying, Version 1.0, T HR TR 13000 ST, NSW Government (Transport for NSW), Sydney, Australia, 2016.*

[6] *NR/L3/TRK/0030 NR_Reinstatement of Absolute Track Geometry* (*WCRL Routes*), no. 1, NR, London, UK, 2008.

[7] *Standardy Techniczne – Szczegółowe warunki techniczne dla modernizacji lub budowy linii kolejowych do predkości $V_{max} \leq 200$ km/h (dla taboru konwencjonalnego) / 250 km/h (dla taboru z wychylnym pudłem) – TOM I – DROGA SZYNOWA – Załącznik ST-T1_A6: Układy geometryczne torów*, PKP Polskie Linie Kolejowe, Warszawa, 2018.

[8] L. Wang et *al*., "Validation and assessment of multi-GNSS real-time Precise Point Positioning in simulated kinematic mode using IGS real-time service," *Remote. Sensing*, vol. 10, pp. 1–19, 2018, doi: 10.3390/rs10020337.

[9] Y. Quan, and L. Lau, "Development of a trajectory constrained rotating arm rig for testing GNSS kinematic positioning," *Measurement*, vol. 140, pp. 479–485, 2019, doi: 10.1016/j.measurement.2019.04.013.

[10] R.M. Alkan, "Cm-level high accurate point positioning with satellite-based GNSS correction service in dynamic applications," *J. Spatial Sci.*, vol. 66, no. 2, pp. 351–359, 2019, doi: 10.1080/14498596.2019.1643795.

[11] W. Domski, and A. Mazur, "Input-output decoupling for a 3D free-floating satellite with a 3R manipulator with state and input disturbances," *Bull. Pol. Acad. Sci. Tech. Sci.*, vol. 67, no. 6, pp. 1031–1039, 2019, doi: 10.24425/bpasts.2019.130885.

[12] S. Wu et *al*., "Improving ambiguity resolution success rate in the joint solution of GNSS-based attitude determination and relative positioning with multivariate constraints," *GPS Solutions*, vol. 24, no. 1, article number: 31, 2020, doi: 10.1007/s10291-019-0943-y.

[13] W. Koc and C. Specht, "Application of the Polish active GNSS geodetic network for surveying and design of the railroad," in *Proc. First International Conference on Road and Rail Infrastructure – CETRA 2010*, Opatija, Croatia, Univ. of Zagreb, 2010, pp. 757–762.

[14] W. Koc and C. Specht, "Selected problems of determining the course of railway routes by use of GPS network solution," *Arch. Transp.*, vol. 23, no. 3, pp. 303–320, 2011.

[15] W. Koc, C. Specht, and P. Chrostowski, "Finding deformation of the straight rail track by GNSS measurements," *Annu. Navig.*, no. 19, part 1, pp. 91–104, 2012, doi: 10.2478/v10367-012-0008-6.

[16] W. Koc, C. Specht, P. Chrostowski, and J. Szmagliński, "Analysis of the possibilities in railways shape assessing using GNSS mobile measurements," *MATEC Web Conf.*, vol. 262, no. 4, p. 11004(1–6), 2019, doi: 10.1051/matecconf/201926211004.

[17] W. Koc, C. Specht, J. Szmagliński, and P. Chrostowski, "A method for determination and compensation of a cant influence in a track centerline identification using GNSS methods and inertial measurement," *Appl. Sci.*, vol. 9, no. 20, p. 4347(1–16), 2019, doi: 10.3390/app9204347.

[18] C. Specht and W. Koc, "Mobile satellite measurements in designing and exploitation of rail roads," *Transp. Res. Procedia*, vol. 14, pp. 625–634, 2016, doi: 10.1016/j.trpro.2016.05.310.

[19] C. Specht, W. Koc, P. Chrostowski, and J. Szmagliński, "The analysis of tram tracks geometric layout based on mobile satellite measurements," *Urban Rail Transit*, vol. 3, no. 4, pp. 214–226, 2017, doi: 10.1007/s40864-017-0071-3.

[20] C. Specht, W. Koc, P. Chrostowski, and J. Szmagliński, "Accuracy assessment of mobile satellite measurements in relation to the geometrical layout of rail tracks," *Metrol. Meas. Syst.*, vol. 26, no. 2, pp. 309–321, 2019, doi: 10.24425/mms.2019.128359.

[21] P. Dąbrowski *et al*., "Installation of GNSS receivers on a mobile platform – methodology and measurement aspects," *Scientific Journals of the Maritime University of Szczecin,* vol. 60, no. 132, pp. 18–26, 2019, doi: 10.3390/jmse8010018.

[22] A. Wilk *et al*., "Research project BRIK: development of an innovative method for determining the precise trajectory of a railway vehicle," *Transp. Oveview – Przegląd Komunikacyjny*, vol. 74, no. 7, pp. 32–47, 2019, doi: 10.35117/A_ENG_19_07_04.

[23] L. Marx, "Satellitengestützte Gleisvermessung – auch beim Oberbau," *EI – Eisenbahningenieur*, vol. 58, no. 6, pp. 9–14, 2007.

[24] Y. Naganuma, T. Yasukuni, and T. Uematsu, "Development of an inertial track geometry measuring trolley and utilization of its high-precision data," *Int. J. Transp. Dev. Integr.*, vol. 3, no. 3, pp. 271–285, 2019, doi: 10.2495/TDI-V3-N3-271-285.

[25] C. Qijin *et al*., "A railway track geometry measuring trolley system based on aided INS," *Sensors*, vol. 18, no. 2, p. 538, 2018, doi: 10.3390/s18020538.

[26] T. Strübing, "Kalibrierung und Auswertung von lasertriangulations-basierten Multisensorsystemen am Beispiel des Gleisvermessungs-systems RACER II," *Schriften des Instituts für Geodäsie der Universität der Bundeswehr München*, *Dissertationen*, Heft 91, 2015.

[27] T. Weinold and A. Grimm-Pitzinger, "Die Lagerung der Gleisvermessungen der ÖBB," *Vermessung & Geoinformation*, vol. 7, no. 3, pp. 348–352, 2012.

[28] *Rail design in Civil 3D*, Autodesk, San Rafael, USA, 2019.

[29] *An application for preliminary and detailed 3D design of rail infrastructure V8i PL*, Bentley Systems, Exton, USA, 2019.

[30] *BIM-ready railway design solution*, CGS Labs, Ljubljana, Slovenia, 2018.

[31] W. Koc, "The method of determining horizontal curvature in geometrical layouts of railway track with the use of moving chord," *Arch. Civil Eng.*, vol. 66, no. 4, pp. 579–591, 2020, doi: 10.24425/ace.2020.135238.

[32] W. Koc, "Design of rail-track geometric systems by satellite measurement," *J. Transp. Eng.*, vol. 138, no. 1, pp. 114–122, 2012, doi: 10.1061/(ASCE)TE.1943-5436.0000303.

[33] A. Wilk, C. Specht, K. Karwowski *et al*., "Correction of determined coordinates of railway tracks in mobile satellite measurements," *Diagnostyka*, vol. 21, no. 3, pp. 77–85, 2020, doi: 10.29354/diag/125626.

[34] A. Wilk *et al*., "Innovative mobile method to determine railway track axis position in global coordinate system using position measurements performed with GNSS and fixed base of the measuring vehicle," *Measurement*, vol. 175, p. 109016, 2021, doi: 10.1016/j.measurement.2021.109016.

[35] A. Wilk, W. Koc, C. Specht, S. Judek *et al*., "Digital filtering of railway track coordinates in mobile multi–receiver GNSS measurements," *Sensors*, vol. 20, p. 5018(1–20), 2020, doi: 10.3390/s20185018.

[36] C. Specht *et al*., "Verification of GNSS measurements of the railway track using standard techniques for determining coordinates," *Remote Sensing*, vol. 12, p. 2874(1–24), 2020, doi: 10.3390/rs12182874.